Quinolinyl Triazole Derivatives-Dominant Inhibitors for Mild Steel in Hydrochloric Acid

Shetty, Nitin Kumar; Tasvi Shetty, Pushpanjali*[+]

Department of Chemistry, Manipal Institute of Technology, MAHE, Manipal-576104, INDIA

ABSTRACT: *Quinolinyl triazole derivatives 4-(4-chlorophenyl)-5-{[(5-chloroquinolin-8-yl)oxy]methyl}-2,4-dihydro-3H-1,2,4-triazole-3-thione (4-4CPCQMT), 4-(3-chlorophenyl)-5-{[(5-chloroquinolin-8-yl)oxy]methyl}-2,4-dihydro-3H-1,2,4-triazole-3-thione (4-3CPCQMT) and 4-(4-fluorophenyl)-5-{[(5-chloroquinolin-8-yl)oxy]methyl}-2,4-dihydro-3H-1,2,4-triazole-3-thione (4-4FPCQMT) are of great importance in pharmaceutical chemistry such as antifungal, antituberculosis, anticonvulsant, anticancer activities, etc. The present work highlights the synthesis of the quinolinyl triazole derivatives ((4-4CPCQMT, 4-3CPCQMTand 4-4FPCQMT). The substituents present and the compounds 4-4CPCQMT, 4-3CPCQMTand 4-4FPCQMT were confirmed by FT-IR and NMR spectroscopy. These compounds having many reactive sites were used as inhibitors for mild steel in 1.0 M hydrochloric acid medium at 303 to 323K. An inhibition study was done by electrochemical measurement. The prevention efficiency is in the order 4-4FPCQMT>4-4CPCQMT>4-3CPCQMT. The surface morphology of the mild steel surface was done using SEM, AFM, and, EDX.*

KEYWORDS: *Mild steel; Inhibitor; Tafel polarization; Electrochemical impedance spectroscopy; Scanning electron microscopy.*

INTRODUCTION

Predominantly used metal in industry and household purposes is mild steel because of its large abundance, low price, and, superior properties [1-2]. The main failure of mild steel in many industries is due to its deterioration in acidic medium, during its cleanings such as pickling, chemical itching, or application such as oil well oxidizing where acids are mainly used. This exposure leads to the dissolution of mild steel because of its high reactivity [3]. These problems have to be taken seriously because mild steel is having high technological applications [4-5]. The best method to decrease metal dissolution or to save the metal from the reactive surroundings is to nullify the reactivity of the environment. This can be done easily by the addition of additives having more rate of attraction on the surface. Many synthesized compounds having many active sites of attraction are largely reported to reduce the aggressiveness of acidic and basic medium in contact with mild steel [6-8]. Many synthesized compounds are eco-friendly in nature [9] The organic compounds with good sites of electrons such as localized or delocalized π electrons O, N, S, and P atoms have been found to be contributed excellent inhibition properties.

The efficiency of the organic compounds depends on the number of active sites present on the metal surface, reactiveness of the environment, type of the metal, its structure, size, and charge density, the tendency to attract,

*** To whom correspondence should be addressed.*
+ E-mail: pushpa.bhat@manipal.edu
1021-9986/2022/8/2650-2667 18/$/6.08

Table 1: Constituents of the mild steel.

Element	Si	Al	Mn	Fe
Composition (weight %)	0.157	0.163	0.496	Balance

projected area (orientations) of the compounds towards the metal surface [10-12]. The glance of literature signifies that many N-heterocyclic compounds such as six-membered rings containing one or more than one N-hetero atom and its derivatives, five-membered rings containing one or more than one N-hetero atom and its derivative, or multiple ring compounds containing one or more than one N-hetero atom and its derivative were proved to be good prohibitor for steel or iron corrosion in the highly reactive acid medium [13-19]. As nitrogen has non bonded pair of an electron in one of the sp^3 hybrid orbitals and seals the active sites on the metal surface either by charge sharing or transferring.

In medicinal chemistry quinoline and its derivatives are largely used to prepare drugs against viruses, bacteria, fungi, depression, etc. It also has predominant biological activities like DNA holding abilities, antitumor, and DNA-doping transporter. Even though a few quinolones and their derivatives are reported to be good deterioration inhibitors for steel in acid medium, no experimental study has been documented on corrosion prevention by quinoline triazole derivatives on mild steel in hydrochloric acid. In our present study, quinoline-based molecular hybrids having mercapto 1,2,4-triazole moiety were synthesized, and studied their corrosion inhibition on mild steel in a 1.0 M hydrochloric acid medium.

EXPERIMENTAL SECTION

Material and preparation of anode

The readings are taken with the rods of mild steel whose composition is given in Table 1. From the mild steel rods, test coupons of desired dimensions were prepared. They were 10 mm in diameter and approximately 20 mm in height. Using cold-setting resin, these test coupons were metallographically mounted up to 10 mm in height. The non-molded circular flat surface of the mild steel was polished using different grades of sandpaper (grades from 600-1200) and, finally, with the help of a disc polisher using small granules of levigated alumina abrasive. Those test coupons were washed with highly purified distilled water, organic impurities are removed by washing with organic solvent and the metal surface is completely dried before keeping it in the corrosive medium.

Preparation of 1.0 M HCl medium

35% hydrochloric acid of Merck Company was mixed with highly pure distilled water to prepare the solution of 2M hydrochloric acid. The strength was confirmed by titration using standard sodium hydroxide using phenolphthalein as an indicator. From the 2M HCl, the solution of 1.0M HCl was prepared whenever readings are taken. The readings are taken by keeping the 50mL (45mL 1.0M HCl and 5mL of DMF) in the thermostat maintained at 303 K, 313 K, and 323 K.

Preparation and characterization of inhibitor

Synthesis of inhibitor

Synthesis of quinolinyl carbothioamide 3(a-c)

An equimolar mixture of quinoline hydrazide **1** (2 mmol) and aryl-substituted isothiocyanate, **2(a-c)** was refluxed in methanol (5 mL). On attainment of the reaction, the content was cooled and filtered the solid formed. The product obtained was directly used for further preparation without recrystallization**.**

Synthesis of quinolinyl triazole 4(a-c):

Quinoline carbothioamide **3(a-c)** (1 mmol) with an aqueous 5% NaOH at 70 °C for 1h to form the title compounds **4(a-c).** When the reaction was completed, the content was cooled and acidified with 6N HCl and crystallized from ethanol to afford pure quinolinyl triazole derivatives **4(a–c)**. The product was purified using recrystallization using methanol.

Spectral Studies of Synthesized Inhibitors

4-(4-chlorophenyl)-5-{[(5-chloroquinolin-8-yl)oxy] methyl}- 2,4-dihydro -3*H*- 1,2,4-triazole -3- thione(4-4CPCQMT) (4a)

Yield: 72 %, m.p-237-238 ºC, IR (cm^{-1}): 3042, 2922, 1601, 1450, 1371, 1108; ^{1}H NMR (400 MHz, DMSO-d_6), δ: 5.12 (s, 2H, O-CH_2), 3.73 (s, 3H, OCH_3), 6.88-6.90 (d, 2H, J = 8.7Hz),7.23-7.25 (d, 2H, J = 7.2Hz), 7.41-7.58 (m, 4H, Ar-H), 8.33-8.36 (d, 1H, J = 8.4Hz),8.86-8.87 (d, 1H, J = 2.8Hz), 14.10 (s, 1H, -NH); ^{13}C-NMR (100 MHz, DMSO-d_6) δ: 55.43, 61.36, 112.00, 114.20, 121.49, 122.06, 125.76, 126.61, 129.17, 129.54, 136.03, 139.87,

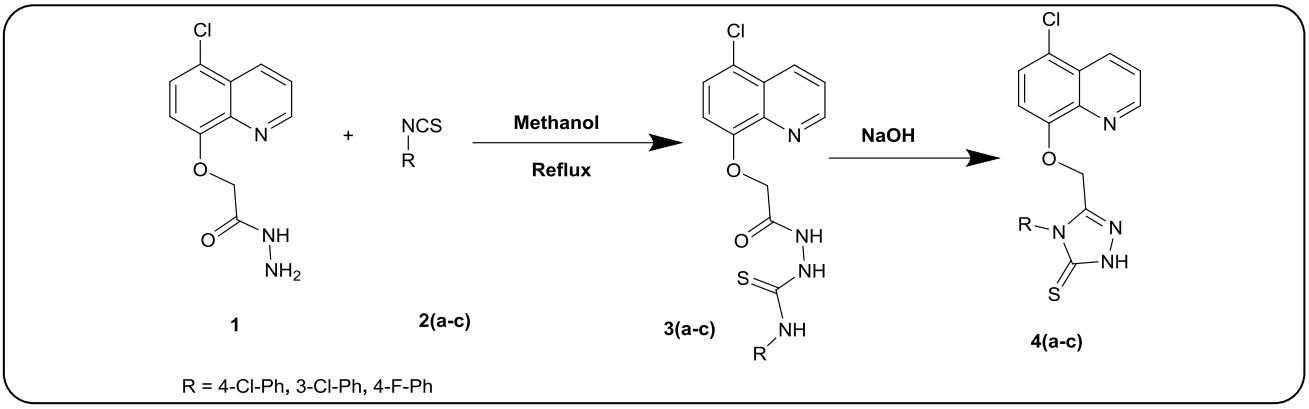

148.46, 149.49, 152.98, 159.65, 168.86; Anal. Calcd for $C_{18}H_{12}Cl_2N_4OS$ (%): C 53.61, H 3.0, N 13.89; Found: C 53.58, H 3.05, N 13.95.

4-(3-chlorophenyl)-5-{[(5-chloroquinolin-8-yl)oxy] methyl}-2,4-dihydro-3*H*-1,2,4-triazole-3-thione(4-3CPCQMT) (4b)

Yield: 65 %, m. p. 230-232 ºC, IR (cm^{-1}): 3038, 2926, 1603, 1452, 1374, 1109; ^{1}H NMR (400 MHz, DMSO-d_6), δ: 5.13 (s, 2H, O-CH_2), 6.98-7.54 (m, 8H), 8.33-8.36 (d, 2H, J = 9.3Hz), 8.87-8.88 (d, 1H, J = 5.7 Hz), 14.14 (s, 1H, -NH); ^{13}C-NMR (100 MHz, DMSO-d_6) δ: 61.46, 112.27, 121.61, 122.01, 126.54, 129.09, 129.12, 130.23, 132.12, 134.13, 136.00, 139.82, 148.12, 149.45, 152.81, 168.67; Anal. Calcd for $C_{18}H_{12}Cl_2N_4OS$ (%): C 53.61, H 3.0, N 13.89; Found: C 53.57, H 3.02, N 13.93.

4-(4-fluorophenyl)-5-{[(5-chloroquinolin-8-yl) oxy] methyl}-2, 4-dihydro-3*H*-1, 2, 4-triazole-3-thione (4-4FPCQMT) (4c)

Yield: 76 %, m.p-219-221 ºC, IR (cm^{-1}): 3039, 2924, 1605, 1457, 1369; ^{1}H NMR (400 MHz, DMSO-d_6), δ: 5.15 (s, 2H, O-CH_2), 6.86-6.88 (d, 2H, J = 8.7Hz),7.22-7.24 (d, 2H, J = 7.2Hz), 7.38-7.56 (m, 4H, Ar-H), 8.32-8.35 (d, 1H, J = 8.4Hz), 8.89-8.90 (d, 1H, J = 2.8Hz), 14.12 (s, 1H, -NH); ^{13}C-NMR (100 MHz, DMSO-d_6) δ: 55.4, 61.3, 112.0, 114.2, 121.5, 122.1, 125.8, 126.7, 129.2, 129.6, 135.9, 139.9, 148.5, 149.5, 153.1, 160.1, 168.9; Anal. Calcd for $C_{18}H_{12}ClFN_4OS$ (%): C, 55.89; H, 3.13; N, 14.48; Found: C, 55.94; H, 3.11; N, 14.53.

Measurements of electrochemical reaction rate

The electrochemical reaction rates of mild steel oxidation and hydrogen ion reduction were measured by using CH Instruments-600D-series purchased U.S. processing beta software. The potentiostat is connected to three electrodes dipped in 45mL of 1.0M HCl and 5mL of DMF with and without 4-4CPCQMT, 4-3CPCQMT, and 4-4FPCQMT respectively. The three electrodes are mild steel, mercury, mercurous chloride saturated electrode, and inert platinum electrode.

Potentiodynamic Polarization Measurements (PDM)

The polarization curves for mild steel oxidation and H^+ reduction were obtained by sweeping the specimen potential from -250 mV in the cathodic direction to +250 mV anodic direction, about the open circuit potential, with 1 mV/s scan rate. The experiments were carried out with and without the addition of optimum concentrations f 4-4CPCQMT, 4-3CPCQMT, and 4-4FPCQMT.

Electrochemical Impedance Spectroscopy

In the electrochemical impedance method, an alternating current signal of small amplitude 10mV and frequency spectrum from 100kHz to 0.01Hz was impressed at the equilibrium potential. The PDM was carried out after the electrochemical impedance method without further polishing the mild steel metal surface. In both measurements, the readings are repeated in 2-3 trials and the average value was recorded.

Surface morphology analysis

The morphology of the mild steel surface, with and without the 4-4CPCQMT, 4-3CPCQMT, and 4-4FPCQMT, was studied by dipping the mild steel coupons of 5mm dimensions in the 1.0M HCl for 2 h. using a JEOL JSM-6380L Analytical Scanning Electron Microscope (SEM). The elements present in the mild steel

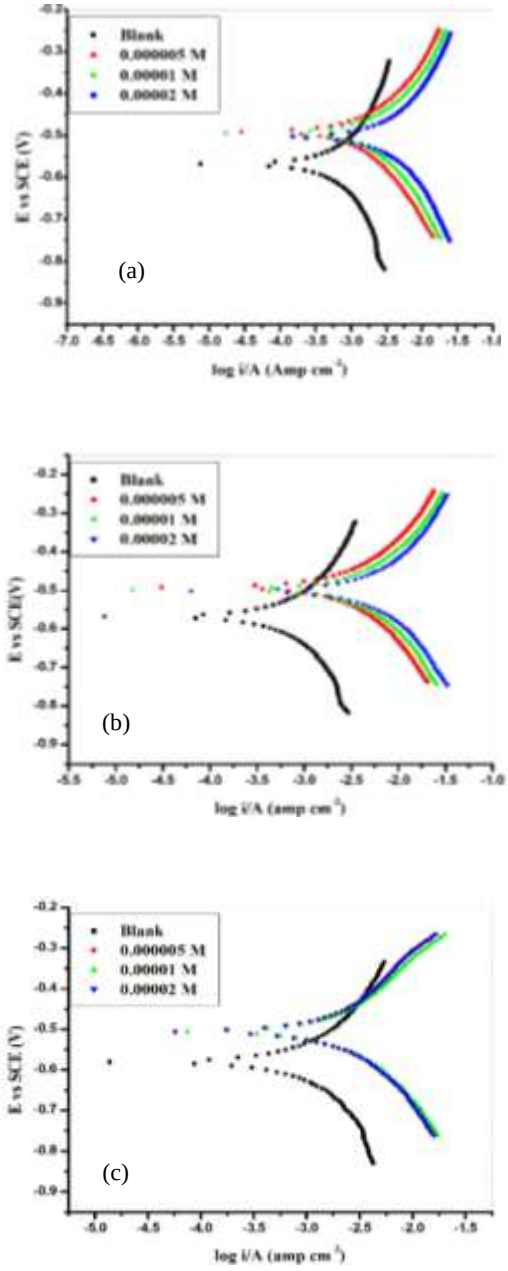

Fig. 1. PDM plots for dissolution of mild steel with varying concentrations of (a) 4-4CPCQMT (b)4-3CPCQMT and (c)4-4FPCQMT in 1.0 M HCl at 313 K.

surface with and without exposure to 4-4CPCQMT, 4-3CPCQMT, and 4-4FPCQMT were studied by Energy–Dispersive X-ray (EDX) spectroscopy. The surface roughness of the mild steel was analyzed using the Atomic Force Microscope (AFM) technique (IB342 Innova model).

RESULTS AND DISCUSSIONS

Potentiodynamic Polarization Results

Fig. 1 shows the cathodic and anodic polarization curves for the destruction of mild steel upon exposing to 1.0M hydrochloric acid medium containing very small amounts 0.5×10^{-4}, $1.0\times10^{-4}$and 2.0×10^{-4}M 4-4CPCQMT or 4-3CPCQMT or 4-4FPCQMT at 303K respectively. From those plots, the PDM parameters were noted.

The Corrosion Rate (CR) related to corrosion current per unit area of the anode was calculated using Eq. (1) [20]:

$$\mathrm{CR(mmY^{-1})} = \frac{\mathrm{i_{corr.}} \times \mathrm{M} \times 3270}{\rho \times \mathrm{Z}} \quad (1)$$

Where 3270 is a conversion factor for the unit of the CR, i_{corr} is a corrosion current per unit area of mild steel (A/cm^2),ρ is the weight per unit volume of the mild steel (7.725 g/cm^3), M is the atomic mass of the mild steel(55.85), and Z is the no of electrons transferred during the anodic reaction of mild steel. For mild steel Z=2.

The % prevention efficiency was evaluated using (2)

$$\mathrm{IE(\%)} = \theta \times 100 \quad (2)$$

Where

$$\theta = \frac{\mathrm{i_{corr.}} - \mathrm{i_{corr.(inh.)}}}{\mathrm{i_{corr.}}} \quad (3)$$

$i_{corr.}$ and $i_{corr.\,(inh)}$ are the corrosion current per unit area of mild steel with and without the introduction of the 4-4CPCQMT or 4-3CPCQMT or 4-3FPCQMT to 1.0M HCl. The results of the PDP study are summarized in Tables 2,3 and 4 respectively [20].

With the introduction of 4-4CPCQMT or 4-3CPCQMT or 4-4FPCQMT to 1.0M HCl corrosion current per unit area was suppressed and prevention efficiency increased. The observed prohibition of 4-4CPCQMT or 4-3CPCQMT or 4-4FPCQMT may be due to the deactivation of reactive sites present on mild steel surfaces by its molecules [20]. These molecules block the surface of mild steel from the corrosive 1.0M HCl. The prevention efficiency of the 4-4CPCQMT, 4-3CPCQMT, and 4-4FPCQMT is in the order of 4-3CPCQMT<4-4CPCQMT < 4-4FPCQMT. This suggests that in 4-4FPCQMT the highly electronegative fluorine atom present in the para position of phenyl ring has a larger tendency to donate non-bonded pair of electrons present in 3p orbitals to vacant 3d orbitals of mild steel. In 4-4CPCQMT has somewhat less electronegative chlorine atom in the para position of the phenyl ring,

Table 2: Results of PDM for corrosion of mild steel in 1.0M HCl with and without 4-4CPCQMT at three temperatures.

Temp. (K)	[4-4CPCQMT] ($\times10^{-5}$M)	$i_{corr.}$ (mA/cm$^{2)}$	C.R. (mmp/y$^{)}$	$-\beta_c$ (mV/dec)	β_a (mV/dec)	$E_{corr.}$ (mV vs SCE)	%I.E
303	0.0	5.68	28.36	497.0	593.6	−502	-----
	0.5	1.13	1.66	612.7	513.3	−495	80.03
	1.0	0.91	2.33	610.6	600.4	−496	83.93
	2.0	0.89	2.76	618.6	544.5	−492	84.34
313	0.0	6.12	41.31	514.3	550.8	−510	-----
	0.5	1.46	2.01	656.9	587.6	−510	76.09
	1.0	1.15	2.80	646.4	494.4	−506	81.21
	2.0	0.96	4.09	644.5	487.3	−505	84.30
323	0.0	7.37	56.25	500.1	478.4	−497	-----
	0.5	2.49	2.27	523.9	496.7	−505	66.21
	1.0	2.11	3.51	541.2	489.7	−506	71.44
	2.0	2.03	6.89	550.3	456.7	−505	72.52

Table 3: Results of PDM for corrosion of mild steel in 1.0M HCl with and without 4-3CPCQMT at three temperatures.

Temp. (K)	[4-3CPCQMT] ($\times10^{-5}$M)	$i_{corr.}$ (mA/cm$^{2)}$	C.R. (mmp/y)	$-\beta_c$ (mV/dec)	β_a (mV/dec)	$E_{corr.}$ (mV vs SCE)	%I.E
303	0.0	5.68	28.36	597.9	633.8	−502	-----
	0.5	0.33	19.51	523.9	563.6	−490	60.4
	1.0	0.21	2.33	501.5	544.4	−492	68.2
	2.0	0.12	2.76	574.1	614.4	−489	76.7
313	0.0	6.12	41.31	526.8	557.9	−510	-----
	0.5	0.38	20.50	487.2	543.4	−494	46.1
	1.0	0.26	2.80	530.9	537.9	−498	64.6
	2.0	0.18	4.09	509.2	506.7	−492	75.1
323	0.0	7.37	41.31	485.7	508.6	−497	-----
	0.5	0.50	2.27	597.9	633.8	−503	43.7
	1.0	0.41	3.51	523.9	563.6	−500	54.7
	2.0	0.32	6.89	501.5	544.4	−494	74.7

Table 4: Results of PDM for corrosion of mild steel in 1.0M HCl with and without 4-4FPCQMT at three temperatures.

Temp. (K)	[4-3CPCQMT] ($\times10^{-5}$M)	$i_{corr.}$ (mA/cm$^{2)}$	C.R. (mmp/y)	$-\beta_c$ (mV/dec)	β_a (mV/dec)	$E_{corr.}$ (mV vs SCE)	%I.E
303	0.0	5.68	28.36	497.0	593.6	−502	-----
	0.5	0.18	11.09	625.9	513.3	−478	96.80
	1.0	0.16	11.99	610.8	600.4	−453	97.16
	2.0	0.13	14.15	684.4	544.5	−437	97.66
313	0.0	6.12	41.31	514.3	550.8	−510	-----
	0.5	0.28	18.26	603.2	587.6	−488	95.40
	1.0	0.22	14.36	601.7	494.4	−477	96.33
	2.0	0.19	18.26	501.7	487.3	−478	96.95
323	0.0	7.37	56.25	500.1	478.4	−497	-----
	0.5	0.55	31.08	551.0	496.7	−484	92.52
	1.0	0.42	26.29	544.5	489.7	−497	94.29
	2.0	0.33	25.29	527.2	456.7	−475	95.56

hence reduced efficiency. But in 4-3CPCQMT the chlorine atom is present in the meta position of the phenyl ring, hence still a reduction in inhibition efficiency due to increased steric hindrance.

As the concentration of 4-4CPCQMT, 4-3CPCQMT, and 4-4FPCQMT rise there will be suppression in mild steel dissolution and reduction of H^+. This may be due to a reduction in the number of active sites of the anode and cathode by blocking inhibitor molecules [21-22].

The anodic polarization curves signify the oxidation of mild steel and the cathodic polarization curves signify the reduction of H^+ showed no change in slope indicating no kinetic barrier effect. These curves are parallel to each other with and without the addition of 4-4CPCQMT, 4-3CPCQMT, and 4-4FPCQMT. This signifies that metal oxidation and H^+ reduction are activations controlled. The cathodic and anodic linear parts (β_a, and-β_c) remained nearly the same with and without 4-4CPCQMT or 4-3CPCQMT or 4-4FPCQMT in 1.0M HCl. This signifies that preventive action of 4-4CPCQMT, 4-3CPCQMT, and 4-4FPCQMT may be due to simple sealing of the available reactive sites on the mild steel surface. In other words, the 4-4CPCQMT or 4-3CPCQMT or 4-4FPCQMT decreases the active sites available for mild steel oxidation and hydrogen evolution and not changing the reaction steps involved in electrochemical reaction at the metal solution boundary. It only causes the passivation of part of the mild steel surface [20, 23].

There was a minor change (less than 85 mV) in the corrosion potential of mild steel (E_{corr}) after the addition of the 4-4CPCQMT or 4-3CPCQMT or 4-4FPCQMT to 1.0M HCl. According to *Li. et al.*, [23], 4-4CPCQMT or 4-3CPCQMT or 4-4FPCQMT are considered as a mixed type of inhibitor. This implies that 4-4CPCQMT or 4-3CPCQMT or 4-4FPCQMT have combined controllers on both mild steel oxidation and H^+ reduction.

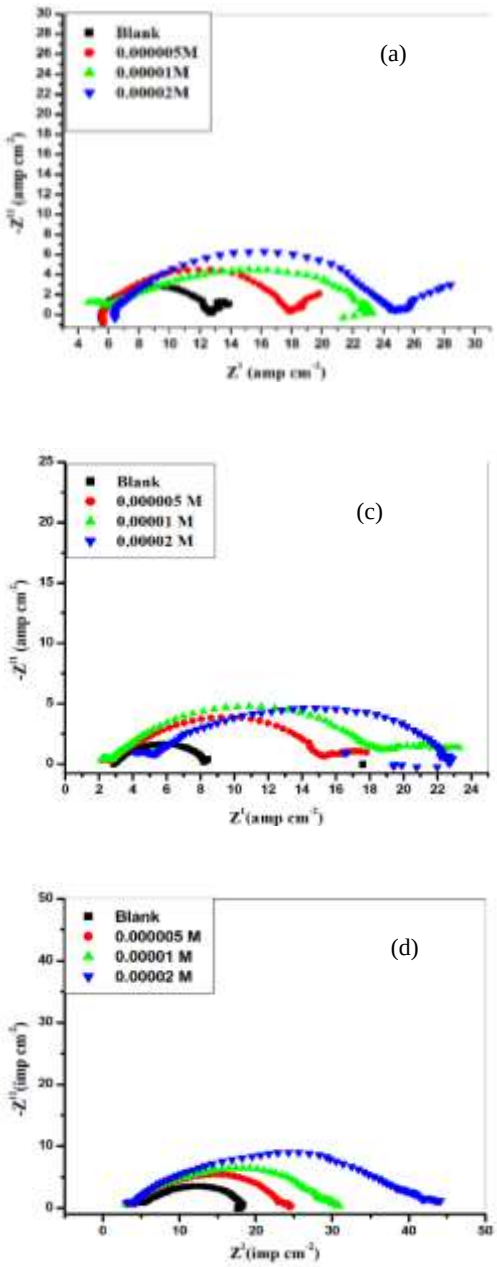

Fig. 2: Nyquist plots for destruction of mild steel in 1.0M HCl with and without (a) 4-4CPCQMT, (b) 4-3CPCQMT, and (c) 4-4FPCQMT at 303K.

Electrochemical Impedance Spectroscopy

Fig. 2 shows the plots of the imaginary part of the impedance against the real part of the impedance for the destruction of mild steel in a 1.0 M HCl with and without 4-4CPCQMT or 4-3CPCQMT or 4-4FPCQMT at 303K. At 313K and 323K, similarly shaped graphs are obtained.

The impedance curves have a half-circle shape at high frequency. This suggests that the reaction involved at the boundary of mild steel and 1.0M HCl involves the exchange of charges and dielectric constant at the electrical double layer. The half circles shrunk with and without the addition of the 4-4CPCQMT or 4-3CPCQMT or 4-4FPCQMT. The depression occurs due to the frequency dispersion, it occurs due to the nonuniform surface formed by the oxide film or blocking of the

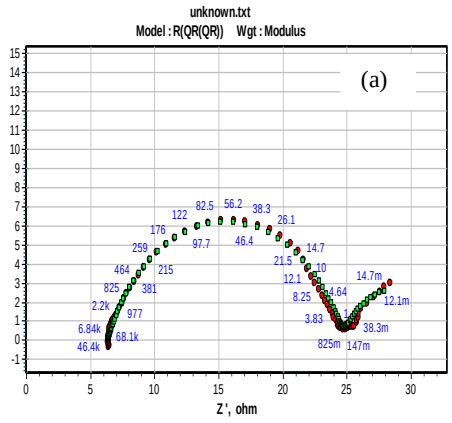

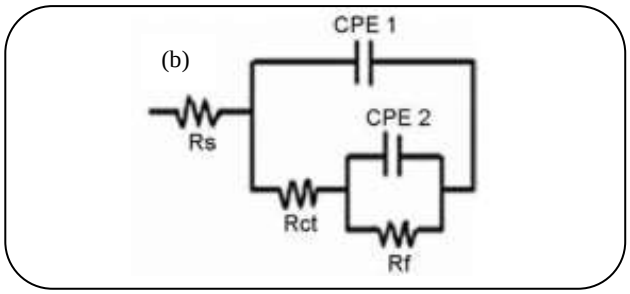

Fig. 3: (a) Impedance data fit for corrosion of mild steel in 1.0M HCl with 4-4CPCQMT or 4-3CPCQMT or 4-4FPCQMT (2×10^{4}M) at 303K. (b) Equivalent circuit.

inhibitors on the metal surface. The diameter of the semicircles enlarged with the addition of more concentrations of 4-4CPCQMT or 4-3CPCQMT or 4-4FPCQMT to 1.0M HCl, which indicates the impedance of the mild steel surface for metal oxidation and reduction of H^+ increases [24-26].

The Nyquist plots are analyzed by putting the impedance data in the Zimp win software 3.21 to get the suitable equivalent circuits. The acceptable equivalent circuit having the least Zai factor is shown in Fig. 3(b) and fitted plots are shown in Fig. 3 (a).

R_s is the resistance of solution present between the electrode, R_{ct} resistance to charge transfer at the metal – 1.0M HCl boundary, constant phase element 1 (CPE_1) the dielectric constant of the electrical double layer, CPE_2 capacitance of the passive film, R_f film resistance. Due to inhomogeneity, the charged layer at the mild steel and solution at the boundary is not a perfect capacitor. Hence it is replaced by CPE [20].

CPE impedance is given by (4)

$$Z = Q^{-1}(iw)^{-n} \quad (4)$$

Q is the proportionality coefficient; $w=2\pi f_{max}$ is the angular frequency and f_{max} is the frequency at which the imaginary component of the impedance is maximum; i is the imaginary number and the exponent factor n is dependent on phase shift. If n = 1, then the CPE behaves like an ideal capacitor. The correction in the capacitance to its real value is calculated using Eq. (5)[20-22].

$$C_{dl} = Q(w)^{n-1} \quad (5)$$

The capacitance (C_{dl}) at the metal electrolyte boundary with and without 4-4CPCQMT or 4-3CPCQMT or 4-4FPCQMT was evaluated from Eq. (6).

$$C_{dl} = 1/2\pi f_{max}.R_p \quad (6)$$

The polarization resistance (R_p) with and without 4-4CPCQMT or 4-3CPCQMT or 4-4FPCQMT was calculated using (7).

$$R_p = R_{ct} + R_f + R_s \quad (7)$$

The dependence of R_p on %IE is given by Eq. (8).

$$\%IE = R_{p(inh.)} - R_p / R_{p(inh.)} \quad (8)$$

$R_{p(inh.)}$ and R_p with and without the addition of the 4-4CPCQMT or 4-3CPCQMT or 4-4FPCQMT to 50mL of 1.0M HCl.

Figs. 2(a), (b), and (c) represents that, R_s by adding or not adding 4-4CPCQMT or 4-3CPCQMT or 4-4FPCQMT to 50mL of 1.0M HCl has the closely same value. By introducing 4-4CPCQMT or 4-3CPCQMT or 4-4FPCQMT to 1.0M HCl R_p value rises and C_{dl} values reduce. This proves the closing of reactive sites present on mild steel surfaces by active molecules of inhibitor. This blocking is possible by the interchange of the polar water molecules or ions at the metal electrolyte boundary by inhibitor molecules. At this region net dielectric, constant diminishes and thickness increases. Therefore by introducing 4-4CPCQMT or 4-3CPCQMT or 4-4FPCQMT to 1.0M HCl capacitance is diminished and resistance to shifting equilibrium potential (R_p) rises at the metal electrolyte boundary. On adding more and more concentration of 4-4CPCQMT or 4-3CPCQMT or 4-4FPCQMT to 50mL of 1.0M HCl resistance to change in equilibrium potential increases and capacitance suppresses. The blocking effect of 4-4CPCQMT or 4-3CPCQMT or 4-4FPCQMT maximizes at 2×10^{-5}M beyond this no change [24].

Table 5: Results of EIS for corrosion of mild steel in 1.0M HCl with and without 4-4CPCQMT at 303K, 313K, and 323K.

Temp. (K)	[4-4CPCQMT]×10^{-5}M	C_{dl} (×10^{-3} F/cm^2)	R_P (ohmcm^2)	%I.E.
303	Blank	4.25	12.0	----
	1.0	2.30	25.0	50.00
	2.0	1.29	28.0	57.14
	4.0	0.73	35.0	65.71
313	Blank	5.47	10.0	----
	1.0	2.64	20.0	50.00
	2.0	1.57	24.0	58.33
	4.0	1.07	28.0	64.29
323	Blank	9.33	8.0	----
	1.0	3.88	15.0	46.67
	2.0	2.28	19.0	57.89
	4.0	1.45	24.0	66.67

Table 6: Results of EIS for corrosion of mild steel in 1.0M HCl with and without 4-3CPCQMT at 303K, 313K, and 323K.

Temp. (K)	[4-3CPCQMT]×10^{-5}M	C_{dl} (×10^{-3} F/cm^2)	R_P (ohmcm^2)	%I.E.
303	Blank	4.25	12.0	----
	1.0	2.68	21.5	44.19
	2.0	1.36	26.5	54.72
	4.0	0.81	31.5	61.90
313	Blank	5.47	10.0	----
	1.0	3.02	17.5	42.86
	2.0	1.89	20	50.00
	4.0	1.20	25	60.00
323	Blank	9.33	8.0	----
	1.0	4.31	13.5	40.74
	2.0	2.83	15.3	47.71
	4.0	1.81	19.3	58.59

This may be due to the saturation of mild steel surface by inhibitor molecules. The impedance parameters are given in Tables 5, 6, and 7. In EIS technique, %I.E. is in the order 4-3CPCQMT < 4-4CPCQMT < 4-4FPCQMT. This signifies that the presence of highly electronegative fluorine atoms increases the blocking of the mild steel surface on exposure to 1.0M HCl.

Causes of change in thermostat temperature

On rising the thermostat temperature from 303K- 323K prevention efficiency of 4-4CPCQMT or 4-3CPCQMT or 4-4FPCQMT reduces. The reason may be deblocking effect or locked molecules of 4-4CPCQMT or 4-3CPCQMT or 4-4FPCQMT leave the reactive sites from the surface of mild steel. The other reason may be a reduction in electrolyte viscosity and increased ionic

Table 7: Results of EIS for corrosion of mild steel in 1.0M HCl with and without 4-4FPCQMT at 303K, 313K, and 323K.

Temp. (K)	[4-4FPCQMT]×10^{-5}M	C_{dl} (×10^{-3} F/cm^2)	R_P (ohmcm^2)	%I.E.
303	Blank	4.25	12	----
	1.0	1.88	30.53	60.69
	2.0	1.02	35.33	66.03
	4.0	0.57	45	73.33
313	Blank	5.47	10	----
	1.0	2.18	24.3	58.85
	2.0	1.31	29	65.52
	4.0	0.88	34	70.59
323	Blank	9.33	8	----
	1.0	3.14	18.5	56.76
	2.0	1.92	22.5	64.44
	4.0	1.37	25.5	68.63

mobility by increasing the thermostat temperature [27]. This deblocking with temperature implies that there will be a weak force of attraction is present between a mild steel and 4-4CPCQMT or 4-3CPCQMT or 4-4FPCQMT molecules. The dependence of temperature on the destruction of mild steel and its prohibition by 4-4CPCQMT or 4-3CPCQMT or 4-4FPCQMT is clearly understood by applying the Arrhenius rate law (9) and transition state Equation (10) for the corrosion rate values recorded by potentiodynamic polarization measurements [17].

$$\ln CR = B - \frac{E_a}{RT} \quad (9)$$

The *B* is an Arrhenius pre-exponential factor; *R* = 8.314 J/mol.K), *T* is thermostat temperature. The graph obtained by taking ln(CR) on Y-axis and 1/T on X-axis gave straight lines with R^2=0.99 and from the -slope×R energy of activation was calculated and is shown in Fig. 4.

$$CR = \left(\frac{RT}{Nh}\right) \exp\left(\frac{\Delta S_a}{R}\right) \exp\left(-\frac{\Delta H_a}{RT}\right) \quad (10)$$

h = 6.626×10^{-34}Js), N =6.023×10^{23}.

The graph obtained by taking ln (CR/T) on Y-axis and 1/T on X-axis gave straight lines and -slope×R gives ΔH_a, [Intercept-lnR/Nh]R gives ΔS_a. The graphs are given in Figs. 5(a), (b), and (c), and the results are tabulated in Table 8.

By introducing 4-4CPCQMT or 4-3CPCQMT or 4-4FPCQMT to 1.0MHCl, E_a upsurges. This may be due to the blocked molecules of 4-4CPCQMT or 4-3CPCQMT or 4-4FPCQMT on mild steel increasing the energy barrier for the metal oxidation or hydrogen evolution [28, 29]. In both, the graphs R^2 nearly equal to one highlights the good dependence of lnCR or lnCR/T on thermostat temperature.

ΔH_a follows a similar trend as E_a. The + value of ΔH_a implies that metal destruction occurs with the absorption of heat and the destruction becomes difficult due to blocking action by molecules of 4-4CPCQMT or 4-3CPCQMT or 4-4FPCQMT [20]. E_a and ΔH_a values for mild steel are high in the presence of 4-4CPCQMT and 4-4FPCQMT and low in the presence of 4-3CPCQMT in 1.0M HCl. This rectifies that the energy barrier formed by 4-4CPCQMT and 4-4FPCQMT molecules is more than by 4-3CPCQMT as they have a greater attraction tendency.

ΔS_a values were large and negative. This rectifies that during the formation of intermediate involved in different steps of mild steel oxidation or hydrogen evolution, the systematicness on the surface of mild steel improved [20-23].

Adsorption conceptions

The capacitance of the electrical double layer present at the mild steel and HCl boundary is reduced by the exchange of polar water molecules by the huge molecules

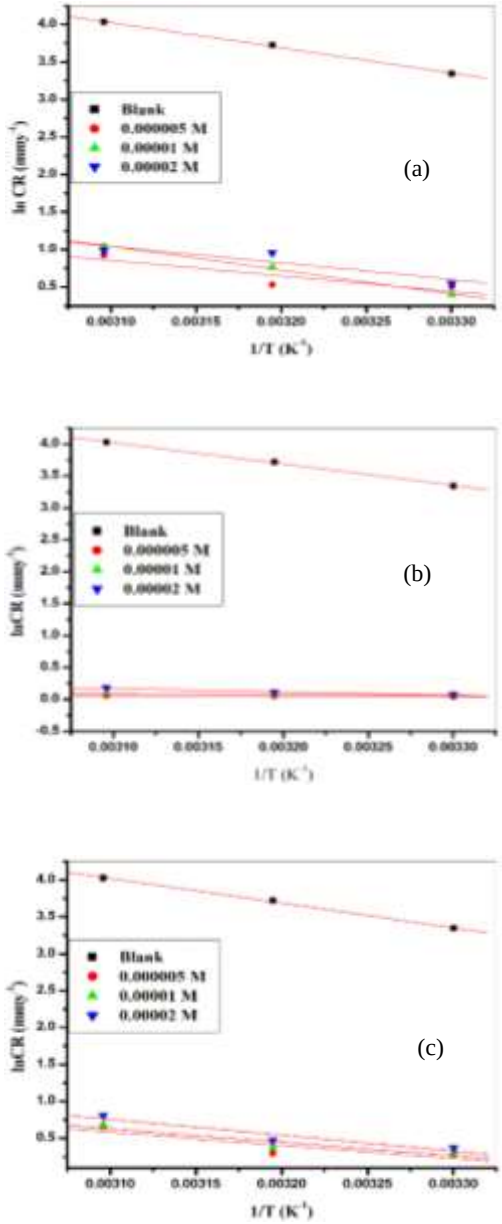

Fig. 4: Arrhenius plots for corrosion of mild steel with different concentrations of (a) 4-4CPCQMT (b) 4-3CPCQMT (c)4-4FPCQMT in 1.0M HCl.

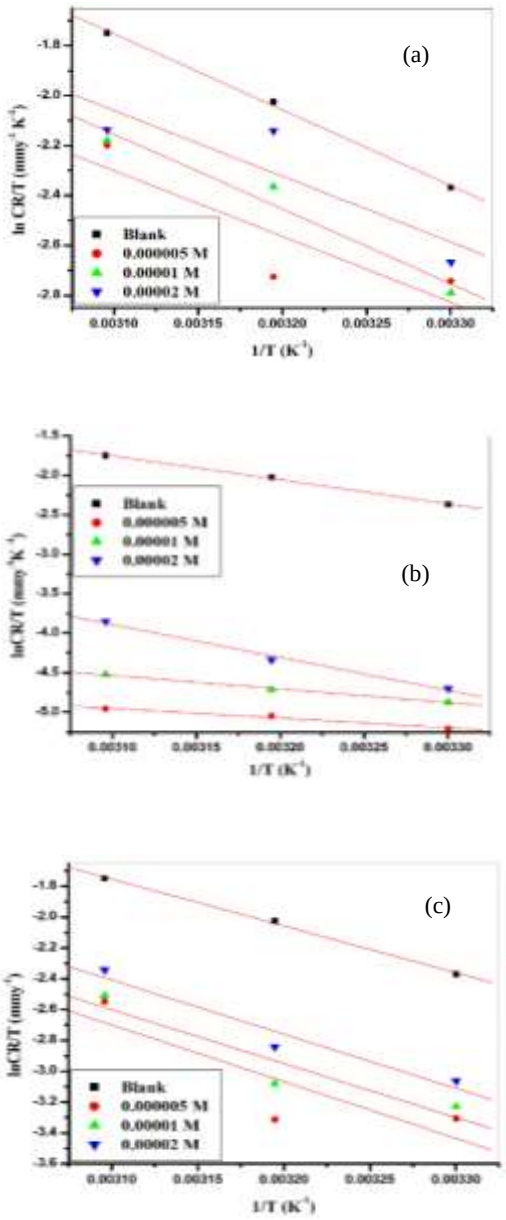

Fig. 5: Graph ln(CR/T) vs. 1/T for corrosion of mild steel in 1.0M HCl with and without (a) 4-4CPCQMT (b) 4-3CPCQMT (c) 4-4FPCQMT.

of 4-4CPCQMT or 4-3CPCQMT or 4-4FPCQMT. Suppression by molecules is presumed to be by adsorption on the mild steel surface. The reaction involved is given in (10) [27].

$$Inh_{(sol)} + nH_2O_{(ads)} \; Inh_{(ads)} + nH_2O_{(sol)} \qquad (11)$$

The intermediate steps involved (a mechanism) in adsorption between the molecules of 4-4CPCQMT or 4-3CPCQMT or 4-4FPCQMT and mild steel can be tracked by adsorption isotherm. This is achieved by equating the fraction of reactive sites present on the metal surface blocked by molecules of 4-4CPCQMT or 4-3CPCQMT or 4-4FPCQMT (θ) to different adsorption isotherm [20]. The suitable isotherm to describe the barrier formation by 4-4CPCQMT or 4-3CPCQMT or 4-4FPCQMT on the mild steel surface is well known Langmuir adsorption isotherm and is given in (12).

Table 8: Activation parameters for 4-4CPCQMT, 4-3CPCQMT, and 4-4FPCQMT.

Name of Inhibitor	[Inh.] ($\times 10^{-5}$M)	E_a (kJ/mol)	ΔH_a (kJ/mol)	ΔS_a (kJ/mol. K)
4-4CPCQMT	0.0	27.88	25.28	−133.72
	0.5	12.23	21.89	−148.78
	1.0	21.82	24.92	−138.18
	2.0	29.44	21.87	−146.86
4-3CPCQMT	0.0	27.88	25.28	−133.72
	0.5	0.65	10.27	−188.18
	1.0	1.24	14.10	−191.54
	2.0	4.34	34.60	−122.64
4-4FPCQMT	0.0	27.88	25.28	−133.72
	0.5	14.80	30.58	−125.16
	1.0	14.95	29.14	−128.82
	2.0	17.73	29.28	−126.79

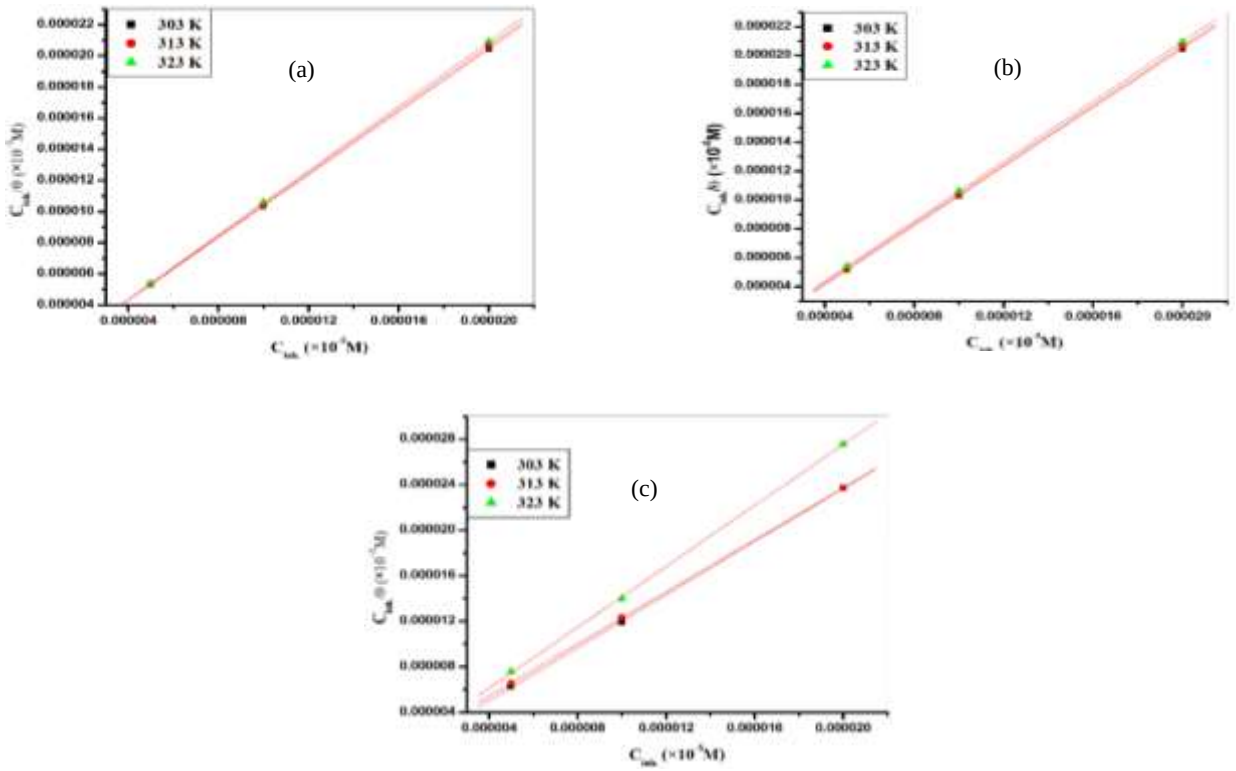

Fig. 6: Langmuir adsorption isotherms for (a) 4-4CPCQMT (b) 4-3CPCQMT and (c) 4-4FPCQMT.

$$\frac{\theta}{1-\theta} = K_{ads.}C \qquad (12)$$

$K_{ads.}$ is the adsorption constant when the system attains equilibrium. By plotting the graph of C_{inh}/θ on Y-axis and C_{inh} on X-axis gave straight lines with an intercept = 1/K which are shown in Fig. 6.

K values were found to be big and the average value of K was 4.1×10^6 and 8.5×10^6 and 1.4×10^6 in the presence

Table 9: Thermodynamic parameters for 4-4CPCQMT, 4-3CPCQMT, and 4-4FPCQMT.

Name of Inhibitor	Temp. (K)	$\Delta G^{\circ}_{ads.}$ (kJ/mol)	$\Delta H^{\circ}_{ads.}$ (kJ mol^{-1})	$\Delta S^{\circ}_{ads.}$ (kJ mol^{-1} K^{-1})
4-4CPCQMT	303	–48.16	–31.74	–0.015
	313	–50.10		
	323	–52.06		
4-3CPCQMT	303	–46.78	–8.14	–0.052
	313	–47.58		
	323	–48.62		
4-4FPCQMT	303	–57.35	–47.90	–0.030
	313	–57.97		
	323	–57.87		

of 4-4CPCQMT or 4-3CPCQMT or 4-4FPCQMT. The huge value of K represents the 4-4CPCQMT or 4-3CPCQMT or 4-3FPCQMT molecules held on the mild steel surface by the firm force of attraction.

The average linear regression coefficient (R^2) for the Langmuir graph was 0.99. This proves the good relationship between C_{inh}/θ on $C_{inh.}$ and closely fitting of adsorption of inhibitors to Langmuir adsorption isotherm. The average slope of straight lines was 1.01 for 4-4CPCQMT or 4-3CPCQMT or 4-3FPCQMT. This proves that adsorbed molecules of 4-4CPCQMT or 4-3CPCQMT or 4-3FPCQMT do not interact with neighboring molecules and form a monolayer on the mild steel surface [20].

K is related to the standard free energy of adsorption ($\Delta G°_{ads.}$) by (13).

$$K = \frac{1}{C_{water}} \exp.\left[\frac{\Delta G^{\circ}_{ads.}}{RT}\right] \quad (13)$$

C_{water}=55.5 mol/L.

$\Delta G°_{ads.}$ Values obtained by using equation (13) are listed in Table 9 [27]. The minus values of $\Delta G°_{ads.}$ Imply that 4-4CPCQMT or 4-3CPCQMT or 4-4FPCQMT molecules are adsorbed without any outside influence and are highly established on a mild steel surface.

The thermodynamic Eq. (14) was used to calculate $\Delta H°_{ads}$ and $\Delta S°_{ads}$.

$$\Delta G^{\circ}_{ads} = \Delta H^{\circ}_{ads} - T\Delta S^{\circ}_{ads} \quad (12)$$

Plotting the graph of $\Delta G°_{ads}$ on Y-axis and T on X-axis gives a straight line with slope = ΔS°_{ads} and intercept= ΔH°_{ads} and are shown in Fig. 7 for 4-4CPCQMT, 4-3CPCQMT, and 4-4FPCQMT respectively. The R^2 value for $\Delta G°_{ads}$ versus T plot 0.99 and the curves are linear, clearly showing the dependence of $\Delta G°_{ads}$ on T and all the

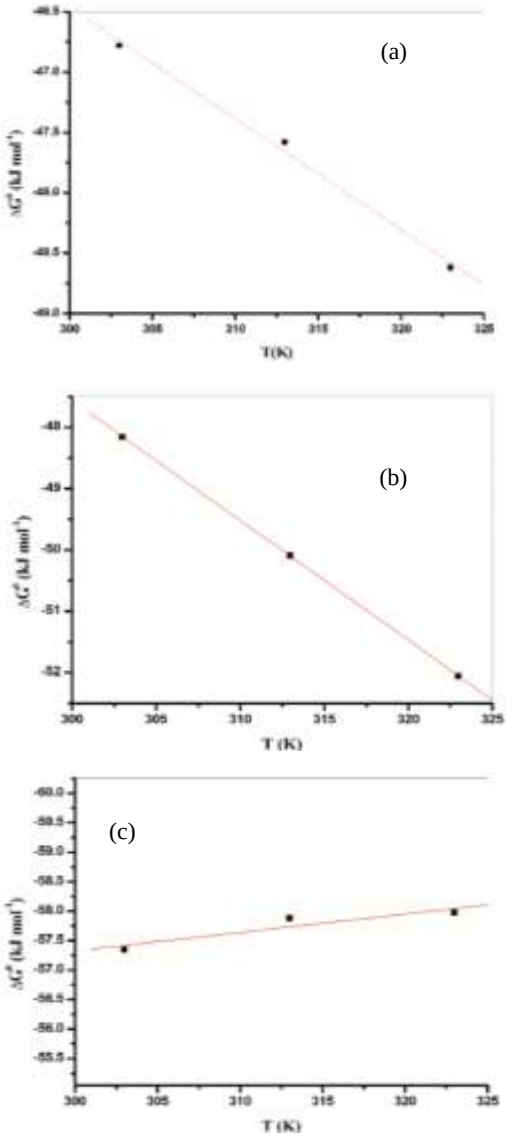

Fig. 7: Plots of $\Delta G°_{ads.}$ vs. T for (a) 4-4CPCQMT (b) 4-3CPCQMT and (c) 4-4FPCQMT on mild steel in 1.0M HCl.

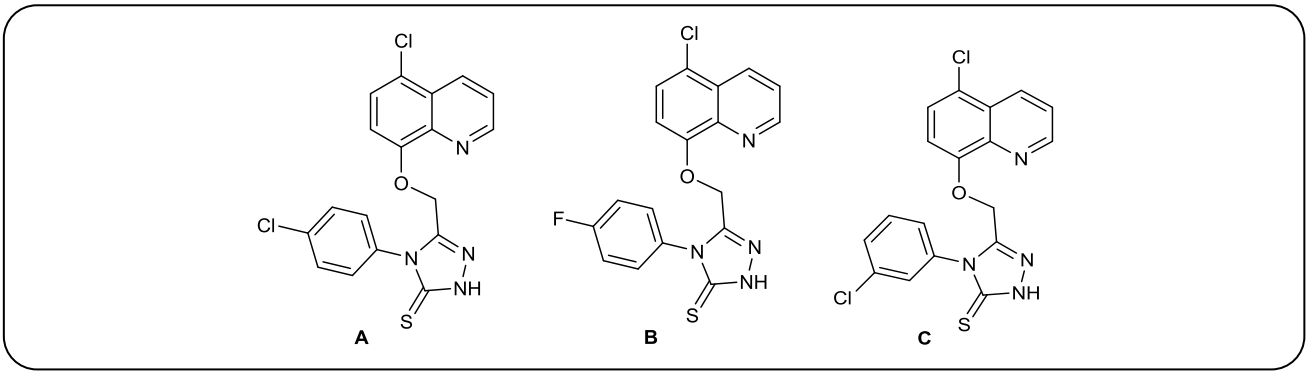

Fig. 8: Structure of (a) 4-4CPCQMT (b) 4-3CPCQMT and (c) 4-3FPCQMT.

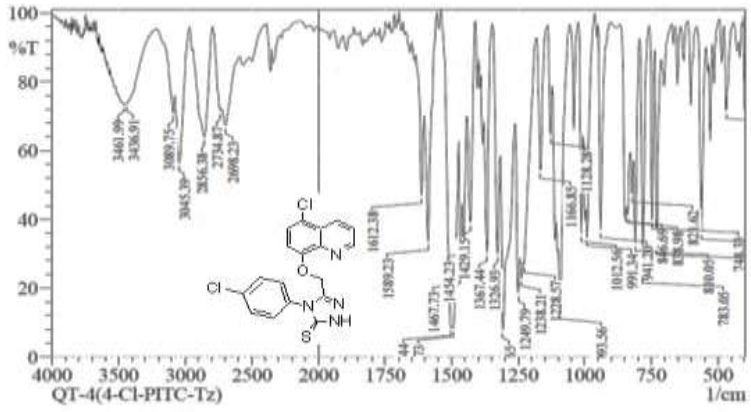

Fig. 9: IR spectrum of the solid residue of Inhibitor.

energy factors are related to each other. $\Delta H°_{ads}$ and $\Delta S°_{ads}$.values are tabulated in Table 9.

$\Delta G°_{ads}$ values for 4-4CPCQMT or 4-3CPCQMT or 4-3FPCQMT on mild steel surface was more than–40 kJ mol^{-1}. This implies the adsorption of 4-4CPCQMT, 4-3CPCQMT, and 4-3FPCQMT on the surface of mild steel is by the chemisorption process[20].

$\Delta H°_{ads.}$values for 4-4CPCQMT, 4-3CPCQMT and 4-3FPCQMT molecules on mild steel were −31.74 kJ/mol, −8.14 kJ/mol, and −47.94 kJ/mol respectively. Which are less than -41.86kJ/mol and in between -41.86kJ/mol and -100kJ/mol respectively[19-20]. This implies that the adsorption of 4-4CPCQMT and 4-3CPCQMT takes place by physisorption and 4-4FPCQMT molecules by the combined effect of physical and chemical adsorption. The $\Delta S°_{ads.}$ value was negative for 4-4CPCQMT, 4-3CPCQMT, and 4-3FPCQMT. This confirms the systematicness increases by adsorption of 4-4CPCQMT or 4-3CPCQMT or 4-3FPCQMT molecules on a mild steel surface.

Mechanism of corrosion and inhibition process

Inhibitor characterization by IR and UV

The structure of Inhibitors is given in Fig. 8.

The FTIR spectra of 4-4CPCQMT, 4-3CPCQMT, and 4-3FPCQMT are shown in Fig. 9. The peaks at 3436, 1612, 1589 cm^{-1} represent the stretching vibrations of the C=C, C=N, and N-H bonds present in the 4-4CPCQMT, 4-3CPCQMT, and 4-3FPCQMT respectively.

The NMR spectrum is shown in Fig.10.

According to the proposed two mechanisms (1) and (2) [28, 29] the wet destruction of iron involving the exchange of two electrons, takes place in two intermediate steps, each step involving the exchange of one electron. One of the slowest steps is considered the rate-determining step (r.d.s.).

In aqueous solutions: Mechanism (1)

$$Fe + H_2O \rightarrow [FeOH]_{ads} + H^+ + e^- \quad (15)$$

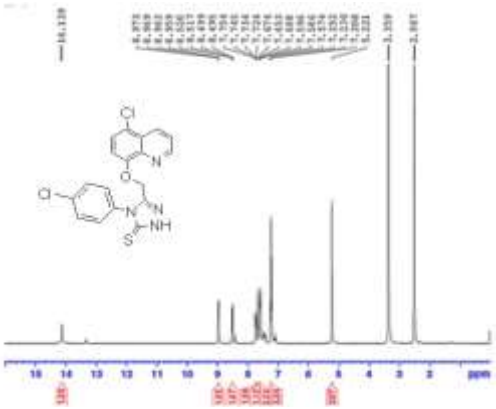

Fig. 11: NMR spectrum of 4-4CPCQMT.

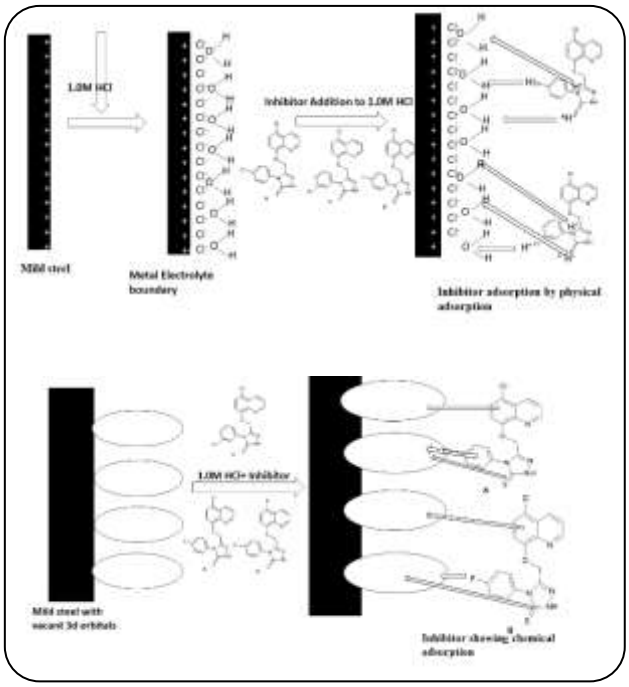

Fig. 12: Inhibitors on mild steel by (a) physical adsorption (b) Chemical adsorption

$$[FeOH]_{ads} \Leftrightarrow [FeOH]^{+}_{ads} + e^{-} \quad \text{(r.d.s)} \qquad (16)$$

$$[FeOH]^{+}_{ads} + H^{+} \Leftrightarrow Fe^{2+} + H_2O \qquad (17)$$

In aqueous solutions containing Cl^-: Mechanism (2)

$$Fe + H_2O + Cl^{-} \Leftrightarrow [FeClOH]^{-}_{ads} + H^{+} + e^{-} \qquad (18)$$

$$[FeClOH]^{-}_{ads} \Leftrightarrow [FeClOH]_{ads} + e^{-} \quad \text{(r.d.s.)} \qquad (19)$$

$$[FeClOH]^{-}_{ads} + H^{+} \Leftrightarrow Fe^{2+} + Cl^{-} + H_2O \qquad (20)$$

The intermediates $[FeOH]_{ads}$ and $[FeClOH]^{-}_{ads}$ involved in r.d.s. are mainly responsible for the destruction of mild steel, according to mechanisms (1) and (2), respectively. From the mechanism, it was observed that in the presence of Cl^- iron dissolution does not occur through the $[FeOH]_{ads}$ intermediate, but through the $FeClOH]^{-}_{ads}$ intermediate. But the two mechanisms can take place simultaneously. Hence, the mild steel surface is having a +ve charge at the anode. This is confirmed by pourbiax diagrams and zero charge potential. Hence it will attract the counter ion Cl- from the aqueous HCl and the double layer of counter ions is formed at the mild steel and HCl boundary [28-29].

The highly electronegative N, Cl, F, or S atoms having nonbonded pair of electrons of 4-4CPCQMT, 4-3CPCQMT, and 4-3FPCQMT may or may not attract H^+ from the aqueous HCl and are available as a neutral molecule or in the form of positively charged species. These positively charged 4-4CPCQMT, 4-3CPCQMT, and 4-3CPCQMT can interact electrostatically with the anodic part of the mild steel surface and adsorb by replacing H_2O resulting in physisorption, These adsorbed inhibitor molecules are larger. They exhibit an umbrella effect by covering both anodic and cathodic areas. Hence, the studied 4-4CPCQMT, 4-3CPCQMT, and 4-3FPCQMT have control over both the reactions involved in metal oxidation and reduction of H^+. The greater prevention efficiency may be due to the donation of π electrons of the aromatic ring or double bond [21-23].

The neutral 4-4CPCQMT or 4-3CPCQMT or 4-3FPCQMT molecules having non-bonded pair of electrons on N, S, Cl, or F atom are donated to the vacant 3d orbital of the Fe atom. Therefore adsorption of 4-4CPCQMT or 4-3CPCQMT or 4-3FPCQMT on mild steel by both but predominantly by chemisorption. The high percentage of chemisorption may be due to the presence of many donor hetero atoms, aromatic rings, and double bonds in the molecule.

Mild steel surface morphology

SEM and EDX analysis

The SEM images of mild steel in 1.0M HCl with and without 4-4CPCQMT or 4-3CPCQMT or 4-3FPCQMT are shown in Fig. 13(a),(b),(c), and (d) respectively.

Table 10: Results of EDX analysis.

Medium	Composition (%)				
	Fe	O	Si	Cl	C
Mild steel in HCl	92.31	7.16	0.37	4.85	-
Mild steel in HCl +4-4CPCQMT(2.0×10^{-5}M)	77.02	7.16	0.38	0.04	15.16
Mild steel in HCl +4-3CPCQMT(2.0×10^{-5}M)	75.02	5.16	0.24	0.05	12.16
Mild steel in HCl +4-4FPCQMT(2.0×10^{-5}M)	79.02	6.16	0.38	0.04	19.30

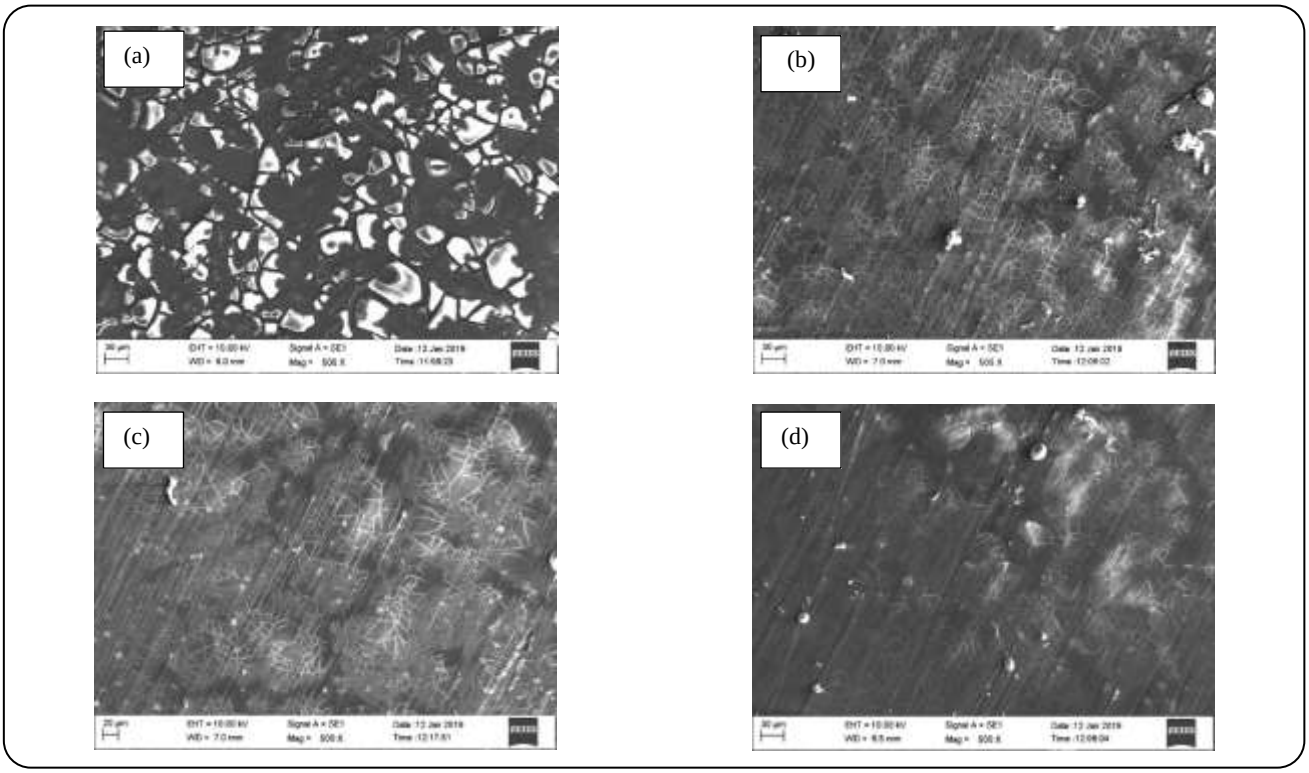

Fig. 12: SEM images of mild steel in: (a) 1.0 M HCl and (b) 1.0M HCl + 4-4CPCQMT (2×10^{-5}M) (c) 1.0M HCl + 4-3CPCQMT(2×10^{-5}M) (d) 1.0M HCl + 4-3FPCQMT(2×10^{-5}M).

The SEM image of mild steel in highly active 1.0M HCl showed a highly uneven surface, which rectifies the mild steel surface undergoing destruction in the HCl [28, 29]. With the introduction of 4-4CPCQMT or 4-3CPCQMT or 4-4FPCQMT to 1.0M HCl, the SEM images of mild steel are smooth. This signifies the reduction in metal oxidation or H^+ reduction as 4-4CPCQMT or 4-3CPCQMT or 4-4FPCQMT molecules lock the active sites present on the mild steel surface. The increased smoothness was observed with 4-4FPCQMT.

The constituents present on the surface of mild steel with and without 4-4CPCQMT or 4-3CPCQMT or 4-3FPCQMT as obtained from the EDX study are given in Table 10. The presence of 4.85 % chlorine on mild steel reflects the interaction of the surface with electrolyte HCl. By adding 2.0×10^{-5}M of 4-4CPCQMTor 4-3CPCQMT or 4-4FPCQMT to 1.0M HCl, the %Cl diminished, and % C elevated to 15.16 %, 19.30%, and 12.16 % respectively. This proves the development of a film of the inhibitor on the metal surface. In the presence of 4-4FPCQMT, the percentage of carbon is more.

Atomic Force Microscopy (AFM)

The 3D-AFM images are given in Fig. 13(a), (b),(c), and (d) respectively.

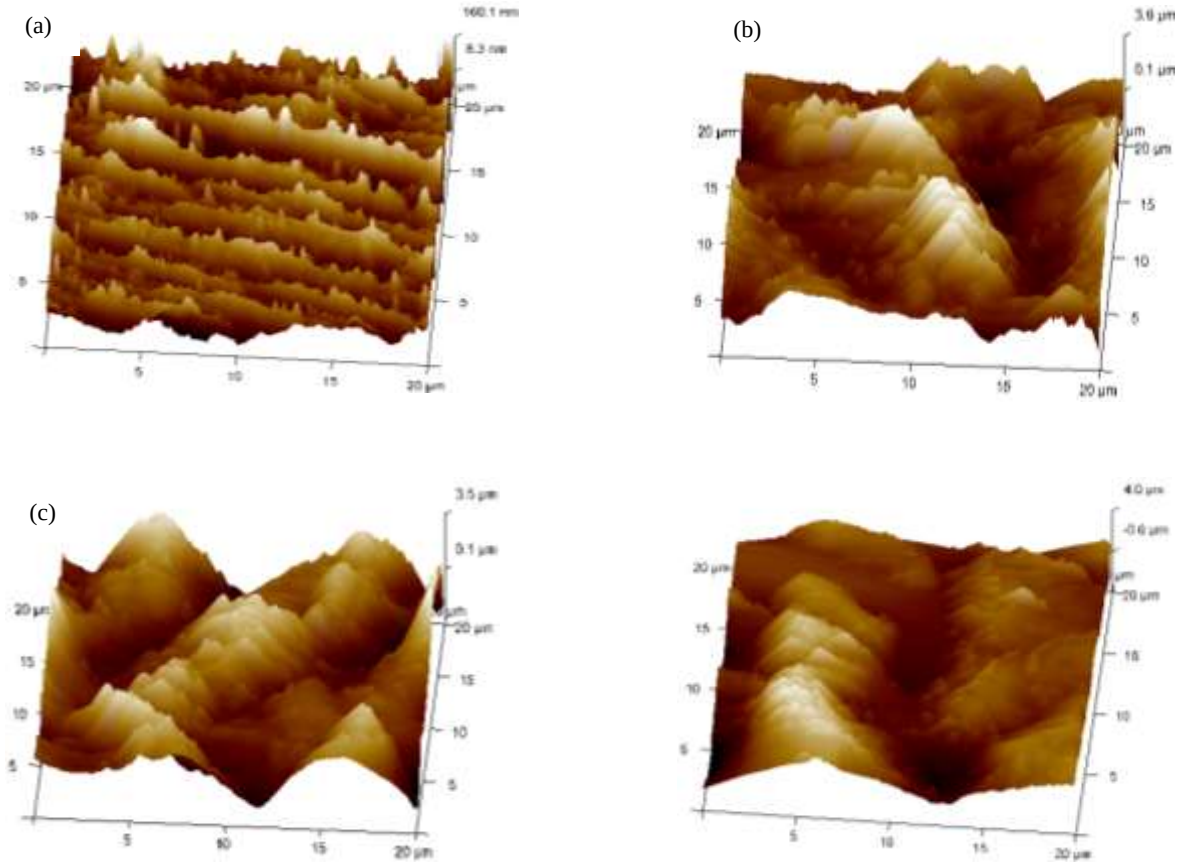

Fig. 13: 3D-AFM images of mild steel in (a) 1.0M M HCl and (b) 1.0M HCl +4-4CPCQMT (2.0×10^{-5}M) (c) 1.0M HCl +4-3CPCQMT (2.0×10^{-5}M) (d)1.0 M HCl +4-4FPCQMT (2.0×10^{-5}M).

Table 11: Results of AFM analysis.

Medium	R_a (nm)	R_q (nm)
Mild steel in HCl	105	86.3
Mild steel in HCl +4-4FPCQMT (2.0×10^{-5}M)	38.2	47.3
Mild steel in HCl +4-3CPCQMT (2.0×10^{-5}M)	30.2	43.3
Mild steel in HCl +4-3FPCQMT (2.0×10^{-5}M)	37.3	45.2

The average surface unevenness (R_a) and the root mean square roughness (R_q) are given in Table 11. R_a and R_q values are suppressed by adding 4-4CPCQMT or 4-3CPCQMT or 4-4FPCQMT to 1.0M HCl. This proves the active sites bound 4-4CPCQMT or 4-3CPCQMT or 4-4FPCQMT molecules reduce the destruction of the mild steel surface. Evenness is improved in the presence of 4-4FPCQMT compared to 4-3CPCQMT or 4-4FPCQMT. The highly electronegative F atom in the para position in 4-4FPCQMT further reduces the corrosion of mild steel in 1.0M HCl. These results are in good agreement with the outcome obtained from the EIS method and PDM.

CONCLUSIONS

- The synthesized compounds are confirmed by IR and NMR spectra.
- In HCl %IE of 4-4CPCQMT,4-3CPCQMT, and 4-4FPCQMT increases with its concentration and decreases with thermostat temperature on mild steel in 1.0M HCl.
- Adsorption of 4-4CPCQMT, 4-3CPCQMT, and 4-4FPCQMT on mild steel mainly by physisorption and 4-4FPCQMT by chemisorption and follows Langmuir's adsorption model.
- 4-4CPCQMT, 4-3CPCQMT, and 4-4FPCQMT function as the mixed type at all its concentrations.

• The prevention efficiency of 4-4FPCQMT is more than 4-4CPCQMT and 4-3CPCQMT

Received : Jul. 8, 2021 ; Accepted : Oct. 11, 2021

REFERENCES

[1] Philip A.S., Fundamentals of Metallic Corrosion, CRC Press, Taylor and Franchis Group, (2006).

[2] Ahmed I., Prasad R., Quarishi M.A., L.I., Thermodynamic and Quantum Chemical Investigator as Corrosion Inhibitor for Mild Steel in HCl Medium, *Corros Sci. (CS)*, 52, 933-942 (2010).

[3] Bentiss F., Lebrini M., Lagrence M., Thermodynamic characterization of Metal Dissolution and Inhibitor adsorption processes in mild steel 2,5-bis(n-thienyl)-1,3,4-thiadiazoles in hydrochloric Acid System. *Corros. Sci.*, **47**: 2915-2931 (2005).

[4] Durnie W.H., DeMarco R., Kinsella B.J., Jefferson A., A Study of Adsorption Properties of Commercial Carbon Dioxide Corrosion Inhibitor Formulations, *J. Electrochem.*, **31**: 1221-1226 (2006).

[5] Geler E., Azambuja D.S., Corrosion Inhibition of Copper in Chloride Solutions by Pyrazole, *Corros Sci.*, **42**: 631-643 (2000).

[6] Hackerman N., Snavely E.S., Jr.Payne J.S., Effects of Anions on Corrosion Inhibition by Organic Compounds, *Electrochem. Soc.*, **113**: 677-686 (1966).

[7] Mercier D.,Barthés-Labrousse M.G., The Role of Chelating Agents on the Corrosion Mechanisms of Commercial Sample of Mild Steel in Alkaline Aqueous Solutions, *Corros. Sci(CS).*, **51**: 339-348 (2009).

[8] Ramesh Kumar S., Danaee I., RashvandAvei M., Vijayan M., Quantum Chemical and Experimental Investigations on Equipotent Effects of (+)R and (−)S Enantiomers of Racemic Amisulpride as Eco-Friendly Corrosion Inhibitors for Mild Steel in Acidic Solution, *J. Molecul. Liq. (JML)*, **212**: 168-186 (2015).

[9] Danaee I., Nikparsa P., Electrochemical Frequency Modulation, Electrochemical Noise, and Atomic Force Microscopy Studies on Corrosion Inhibition Behavior of Benzothiazolone for Steel API X100 in 10% HCl Solution, *J. Material. Eng. and Perfor.(JMEP)*, **28**: 5088-5103 (2019).

[10] Bajat J.B.,Miškovic Stankovic V.B., Kacˇarevic. Popovic Z., Corrosion Stability Of Epoxycoatings on Aluminum Pretreated by Vinyltriethoxysilane, *Corros. Sci. (CS)*, **50**: 2078–2084 (2008).

[11] Sanyal B., Organic Compounds Corrosion Inhibitors in Different Environments, A Review, *Progs. in Organ. Coat (POC)*, **9**: 165-236 (1981).

[12] Ozcan M., Solmaz R., Kardas G., Dehari I., Adsorption Properties of Barbiturates as Green Corrosion Inhibitors of Mild Steel in Phosphoric Acid Colloids Surface, *Physiochem. Eng. Aspects (PEA)*, **325**: 57-63 (2008).

[13] Popova A., Christov M., Vasilev A., Mono and di Cationic Benzothiazolic Quaternary Ammonium Bromides as Mild Steel Corrosion Inhibitors, Part 2, Electrochemical Impedance and Polrisation Resistance Results, *Corros. Sci. (CS)*, **53**: 1771-1777 (2011).

[14] Renata B.O., Elanine M.S.F., Rodrigo P.P.S., Anderson A.A., Antoniana U.K., Carlos L.Z., Synthesis and Antimalarial Activity of Semicarbazone Derivatives, *Europ. Medi. Chem. (EMC)*, **43**: 1984-1988 (1984).

[15] Kalpana B., Hansung K., Gurmeet S., Inhibiting Effects of Butyl Triphenyl Phosphonium Bromide on Corrosion of Mild Steel in 0.5 M Sulphuric Acid Solution and its Adsorption Characteristics, *Corros. Sci. (CS)*, **50**: 2747-2754 (2008).

[16] Sudheer M., Quraishi A., 2-Amino-3,5-dicarbonitrile-6-thio-pyridines: New and Effective Corrosion Inhibitors for Mild Steel in 1 M HCl, *Ind. Eng. Chem. Res. (IECR)*, **53**: 2851-2859 (2014).

[17] Ahmed S.K., Ali W.B., Khadom A.A., Synthesis and Investigations of Heterocyclic Compounds as Corrosion Inhibitors for Mild Steel in Hydrochloric Acid, *Int. J. Ind. Chem. (IJIC)*, **10**: 159-173 (2019).

[18] Danaee I., Nikparsa P., Khosravi-Nikou M.R., Eskandari H., Nikmanesh S., Density Functional Theory and Electrochemical Noise Analysis of Corrosion Inhibition Behavior of N,N'-bis(1-(3,5-dihydroxyphenyl)ethylidene)propane-1,3-diamine on Steel in HCl Solution, *Protect. Metal. Physical Chemist. Surfac. (PMPC)*, **55**: 1000-1013 (2019).

[19] Danaee I., Gholami M., RashvandAvei M., Maddahy M.H., Quantum Chemical and Experimental Investigations On Inhibitory Behavior of Amino-Imino Tautomeric Equilibrium of 2-aminobenzothiazole on Steel Corrosion in H2SO4 Solution, *J. Indust. Eng. Chem. (JIEC)*, **26**: 81-94 (2015).

[20] Mansfeld F.B., "Corrosion Mechanisms", Marcel Dekkar, New York, 165-209 (1987).

[21] Mansfeld F., Lin S., Kim K., Shih H., Pitting and Surface Modification of SiC/Al. *Corros. Sci. (CS)*, **27**: 997-1000 (1987).

[22] Mansfeld F., Lin S., Kim K., Shih H., Electrochemical Impedance Spectroscopy as a Monitoring Tool for Passivation and Localized Corrosion of Al Alloys, *J. Mater. Corros .(JMC)*, **39**: 487-492 (1988).

[23] Li W.H., Q.He Q., Pei C.L, Hou B.R., Some new Triazole Derivatives as Inhibitors for Mild Steel Corrosion in Acid Medium, *J. Appl. Electrochem. (JAE)*, **3**: 289-295 (2008).

[24] Ross Macdonald J., "Impedance Spectroscopy", John Wiley and Sons, Inc., 2nd ed., (1987).

[25] Alves V.A., Brett C.M.A., Characterisation of Passive Films Formed on Mild Steels in Bicarbonate Solution by EIS, *Corros. Sci. (CS)*, **33**: 203-210 (1992).

[26] Bessone J.B., Salinas D.R., Mayer C., Ebert M., Lorenz W.J., An EIS Study of Aluminum Barrier-Type Oxide Films Formed in Different Media, *Electrochem. Acta. (EA)*, **37**: 2283-2290 (1992).

[27] Mansfeld F., Bertocci U., Electrochemical Corrosion Testing, American Society for Testing and Materials, (1979).

[28] Awady A.A., Abd-El−Nabey B.A., Aziz S.G., Thermodynamic and Kinetic Factors in Chloride Ion Pitting and Nitrogen Donor Ligands Inhibition of Mild Steel Metal Corrosion in Aggressive Acid Media, *J. Chem. Soc. (JCS)*, **89**: 795−802 (1993).

[29] Shen C., Wang S., Yang H. Long K.Wang F.., Corrosion Effect of Allylthiourea on Bulk Nanocrystalline Ingot Iron in Diluted Acidic Sulphate Solution, *J. Electrochem. Acta (JEA)*, **52**: 3950-3957 (2007).